# High resolution observations of the thermal SZ effect on galaxy clusters

***Coordinators*:** J.F. Macías-Pérez (LPSC), B. Comis (LPSC), E. Pointecouteau (IRAP)
***Team***: R. Adam (LPSC), N. Aghanim (IAS), M. Arnaud (CEA), F.X. Desert (IPAG), M. Douspis (IAS), F. Mayet (LPSC), P. Mauskopf, J.B. Melin (CEA), L. Perotto, G. Pratt (CEA), .....

We describe here the NIKA2 Guaranteed Time Large Program dedicated to high resolution observations of clusters of galaxies at intermediate and high redshift via the thermal Sunyaev-Zeldovich (tSZ) effect for a total of 300 hours. NIKA2 is well adapted for those observations because of its large number of high sensitive detectors at two frequency bands (150 and 260 GHz) and its large field of view (6.5 arcmin) given the 30 m resolution (18.5 and 11 arcsec for the NIKA2 frequencies). We intend to observe a large sample of clusters of galaxies (above 50) with redshift between 0.5 and 1.5 to make it cosmologically representative. The main output of the program will be the study of the redshift evolution of the cluster pressure profiles as well as of the scaling laws relating cluster observational parameters, Y (integrated Compton parameter), Yx (X-ray mass proxy), and T (temperature) for example, to their mass. This will be achieved by combining the NIKA2 data with ancillary data including X-rays and optical observations and will lead to significant improvements on the use of clusters of galaxies to draw cosmological constraints.

## 1. Scientific context

As the largest gravitationally collapsed objects, clusters of galaxies represent the last step of the hierarchical gravitational process of structure formation. Therefore their abundance and evolution are strictly related to the power spectrum of the primordial density fluctuations, but also to the other cosmological parameters, all along the history of our Universe.

Clusters are mainly made up of dark matter (85%), while most of the baryons are present as a diffuse gas, the Intra-Cluster Medium (ICM), hot ($10^6$ – $10^8$ K) and completely ionized due to the incredibly high masses characterising this kind of structures ($10^{13}$ – $10^{15}$ $M_{Sun}$). Since the ICM is a very good tracer of the dark matter distribution, ICM observables can provide a valuable tool for cosmological investigation with clusters, as long as we are able to convert them into mass estimates. From baryonic observables the total mass can be inferred through scaling relations, which corresponds to power laws obtained in a simplified scenario in which gravity is the only process driving cluster evolution. At present, the systematic uncertainties affecting the observable to mass relations represent the limit for cluster-derived cosmological constraints.

Due to its physical state, the ICM is responsible of a secondary anisotropy of the Cosmic Microwave Background (CMB), which is the thermal Sunyaev-Zel'dovich (SZ) effect. Through their path toward us, CMB photons interact with free hot electrons in the ICM. After this interaction a fraction of CMB photons is moved to higher energies, with a resulting flux decrement (increment) at frequencies below (above) 217 GHz. The amplitude of the deformation is proportional to the integral of the pressure of the electron population along the line of sight. While optical and X-ray cluster signals are affected by cosmological dimming, this is not the case for the tSZ cluster signal. Therefore the tSZ effect allows us to detect and study cluster of galaxies at high redshifts, where their number and distribution is the most sensitive to the underlying cosmology.

In the last few years, tSZ-selected cluster catalogues containing hundreds of candidates have finally been produced, with arcmin resolution, by the South Pole Telescope (SPT, Reichardt et al. 2013), the Atacama Cosmology Telescope (ACT, Hasselfield & ACT Collaboration 2013), the Planck Satellite (Planck Collaboration 2013) and APEX-SZ (Bender et al. 2014). The use of tSZ-selected cluster samples for cosmological purposes requires the understanding of how matter is distributed and the evaluation of the scatter that disturbed systems may introduce in the tSZ integrate flux (Y) to total cluster mass (M) relation. The Planck, ACT, SPT and APEX-SZ resolutions only allow detailed study of spatial distribution of low redshift clusters ( $z < 0.2$). Therefore, high angular resolution measurements of cluster pressure profiles are a mandatory step for precise cluster cosmology. Moreover, pressure profiles – $P_e(r)$ – with spatial resolution comparable to those of X-ray derived electron densities – $n_e(r)$ – can also be used to study the cluster radial distribution of temperature – $T_e(r) \propto Pe(r)/ne(r)$ –

and entropy – K(r) ∝ Pe(r)/ne(r)5/3–, which are essential to unveil the cluster thermodynamic history.

## 2. Main scientific goals

Clusters grow by constant smooth accretion and violent merger events. This mechanisms driving the growth of structures impact cluster content, and thereby this complex accretion history imprint the physical state and properties of the hot intra-cluster gas. Furthermore feedback from galaxy formation (through AGN and SFR/SN) impacts the properties of the gas. It injects energy within the ICM which is known to counter balance the gravitational radiative cooling of the hot gas. This energy injection also modifies the thermodynamical state of the ICM.

We have now a fairly good view of properties for the hot ICM gas in the local Universe, mainly yredshift below 0.5. This has been possible because of recent tSZ measurements that are a powerful diagnostic of the ICM physical state. Indeed the tSZ effect is directly proportional to the thermal pressure integrated along the line of sight. Measuring the (radial) distribution of the SZ signal in clusters directly provide this of the thermal pressure of the ICM. By contrast X-ray measurements are sensitive to the square of the gas density and the root square of the temperature. We present in Figure 1 recent measurements of the stacked cluster radial pressure profile using tSZ observations with PLANCK, BOLOCAM and SPT, and X-ray estimates. From the left plot we can notice that the tSZ measurements are in good agreement but are not able to sample the inner part of the the clusters where important differences are expected between relaxed clusters, which present a Cool Core (CC), and disturbed ones (non- CC). This is more obvious in the right panel where X-ray estimates are presented for CC and non-CC. High resolution tSZ observations are needed for a better understanding of the inner part of cluster pressure distribution and to obtain temperature and entropy profiles.

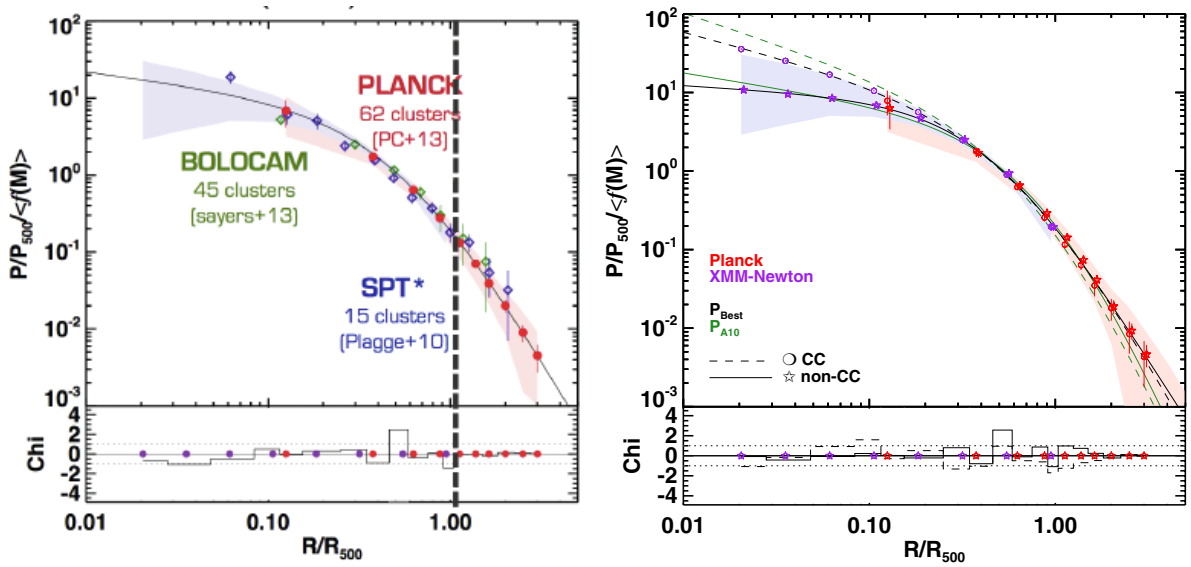


**FIG 1**- Right: normalized mean radial thermal pressure profile of clusters as measured by various tSZ experiments including PLANCK, BOLOCAM and SPT. Left: PLANCK measured cluster pressure profile compared to X-ray estimates from XMM-Newton including Cool Cores (CC) and non-CC clusters.

In addition, we still need to investigate how cluster properties evolve with time in order to understand the mechanisms ruling the formation and the evolution of structure.
The investigation of the physical state of group un cluster with redshift will thus help us to assess the evolution involved by the cluster accretion history, the process of in a gravitationally bound system and by the co-evolution between the baryonic component of clusters, i.e., the hot intra-cluster gas and the cluster galaxies. Carrying such a study over a population of high redshift

clusters will allow to quantify whether the thermal content and its distribution evolve as massive halos continue to growth through accretion and merger. Such measurement will be only possible thanks to the high sensitivity and high spatial resolution tSZ observations. As discussed below NIKA2 is an ideal instrument to carry such observations.

Furthermore, the natural combination of direct observables of the intra-cluster hot gas (i.e., SZ and X-ray measurements) as well as of the dark matter distribution (i.e, optical weak lensing measurements), will allow a full physical characterisation of the (radial) distribution of the physical properties of clusters including pressure, entropy, gas mass, total mass, gas fraction and clumpiness of the gas. Indeed, the tSZ signal directly provides the gas pressure, where the X-ray data delivers the gas density squared and temperature. The combination of the two observables is the only way to provided an unbiased estimate of the entropy and clumpiness of the gas. In addition, weak lensing measurements will provide complementary measurements of the dark matter distribution and total mass of the cluster with totally independent systematics.

Global quantities will derived from 1D (radial profiles) and 2D (maps) analysis in to order to provide further constraints on the evolution of clusters scaling relations (Y-Yx, M-Y, S-Y, etc). Furthermore, the combination of the SZ and X-ray data to optical/NIR observations of the cluster galaxies will further help to investigate the connection between galaxy properties (luminosity function, SFR, stellar mass) and these of the ICM, and thereby bring constraints on feedback mechanisms at play within clusters.

These in depth investigations over a large redshift range will bring detailed insight of the properties of clusters over more than 3 Gyr, allowing us to understand the processes driving the physical evolution of massive halos in the universe.

### 3. NIKA2 specifics for SZ observations

The NIKA2 camera is particularly well adapted for high resolution observations of the tSZ effect on cluster of galaxies:

a) it operates simultaneously at two frequency bands: 150 and 260 GHz. As shown on the bottom panel of Figure 2 we expect for 150 and 260 GHz a negative and a positive distortion of the CMB spectrum producing a very distinctive cluster signal on the observed maps. The latter is demonstrated on the right panel of the figure where we present Planck satellite observations of a cluster of galaxies at 143, 217 and 353 GHz.

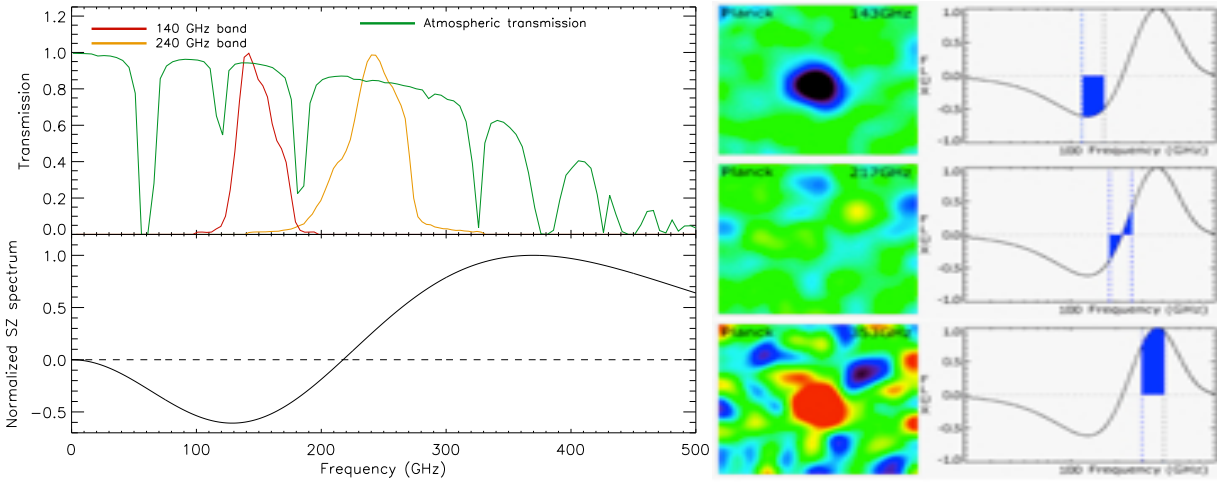


**FIG 2** - Left: On the top plot we present the bandpasses of the current NIKA KIDs arrays at 140 (red) and 240 (orange) GHz and the atmospheric transmission at IRAM. The bottom plot shows the expected CMB spectral distortion induced by the tSZ effect. Right: Maps of a cluster tSZ signal as measured by the Planck satellite at 143, 217 and 353 GHz, and expected CMB spectral distortion.

b) NIKA2 is made of arrays of thousands of high sensitive Kinetic Inductance Detectors (KIDs). In particular we expect a sensitivity in Compton parameter units of 1.13 x$10^{-4}$ per hour and per beam. This should allow us to obtain reliable tSZ detections of clusters of galaxies in few hours.
c) NIKA2 coupled to the IRAM 30 m telescope should allows us to map clusters of galaxies to a resolution of typically 12 to 20 arcsec within a 6.5 arcmin diameter FOV. This is well adapted for medium and high redshift clusters for which we expect typical angular sizes of about 6-11 arcmin as shown on the left panel of Figure 3.

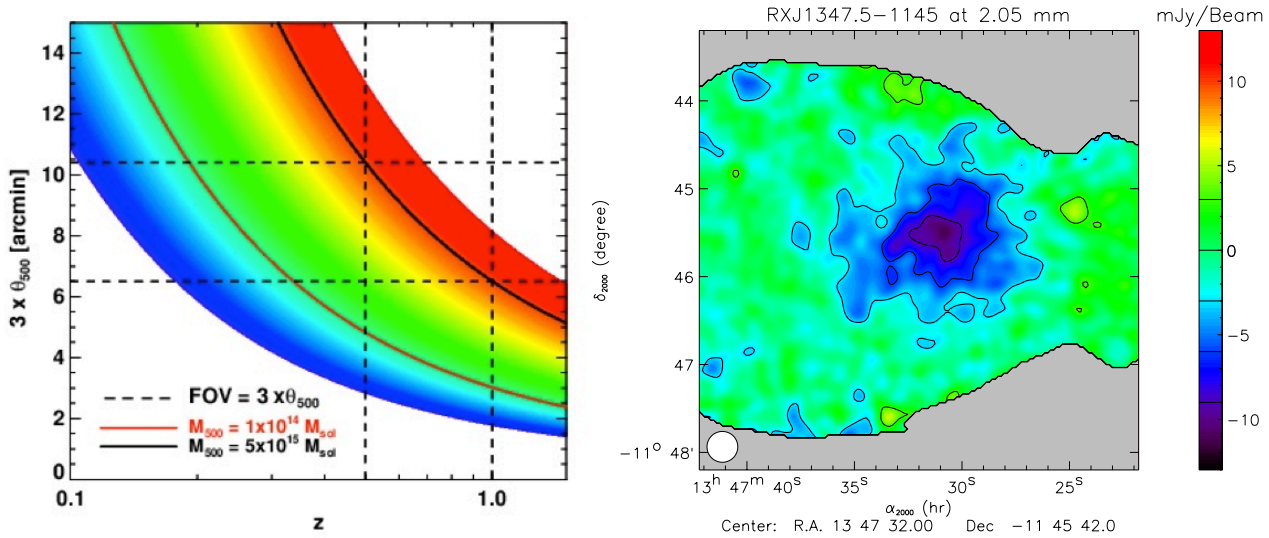


**FIG 3.** Left: evolution of the expected cluster angular size (3 x $\Theta_{500}$) with redshift for a large range of masses. The dashed lines show the FOV required to fully observe a cluster of 5 $10^{15}$ $M_{SUN}$. Right: NIKA map of the tSZ effect at 140 GHz for the RXJ1347.5-1145 cluster at a redshift of 0.45.

The interest of NIKA2 for tSZ observations of clusters of galaxies has already been partially demonstrated by the results of NIKA, which is a prototype instrument operated at the IRAM 30 m telescope with two frequency bands (140 and 240) and 300 KIDs in total. This is shown on the right panel of Figure 3 where we present a 140 GHz tSZ map of the RXJ1347.5-1145 cluster.

It is important to compare the NIKA2 instrument to other existing and planned instruments for high resolution tSZ observations. For this purpose we list below the main characteristics for the most relevant ones:
- BOLOCAM: 144 bolometer arrays operated at the 10 m CSO telescope at 140 and 268 GHz, with 58 and 31 arcsec resolution, over a 8 arcmin diameter FOV.
- MUSTANG/GBT: 64 element bolometer array operating at 90 GHz on the 100 m GBT telescope with a resolution of 8.5 arcsec
- CARMA: 23-element multi-frequency interferometer at 31, 86 and 90 GHz

## 4. Target selection

The main objective of this program is to obtain high resolution tSZ observations of a cosmological representative sample of clusters of galaxies at intermediate and high redshifts, z > 0.5, to study the evolution of cluster physical properties across cosmic times.
In order to fulfill this objective given the limited total observing time, 300 hours, we consider the following target selection criteria:

- relaxed clusters
- clusters from already existing tSZ based cluster samples and in particular from the Planck, ACT and APEX-SZ samples for which we already have estimates of the total tSZ flux (see Figure 4 for details)
- limit sample to clusters in the redshift range from 0.5 to 1.5
- reliable tSZ mapping for each cluster should not exceed 4 hours of on target observations so that the total number of observed cluster is larger than 50

- clusters observed in X-rays (by XMM or Chandra)
- clusters for which weak lensing information is available
- include backup objects

***Ancillary data***

The previous selection criteria rely on the use of ancillary complementary data and existing cluster sample follow-up observations.

For the former we will consider X-ray data coming mainly from XMM and Chandra, but also from Rosat and eRosita. In terms of lensing we will mainly rely on the HST CLASH sample (Postman et al) that provide high quality lensing data and follow-up for 25 clusters. Furthermore we will use the ACCEPT follow-up program of the Chandra cluster sample. Radio observations will be needed to identify strong radio sources in the cluster center. Finally, we will also use IR data from Hershel, Spitzer and IRAS to study contamination from foreground IR sources.

In terms of follow-up programs we will use data from the XMM program “Unveiling the most massive clusters at z> 0.5 with Planck and XMM-Newton” (PI. M. Arnaud), the ITP/ESO program “Systematic follow-up of newly discovered Planck cluster candidates” (PI J.A. Rubino-Martin and N. Aghanim), and the CFHT/Megacam program “The most massive clusters across cosmic time” (PI G.Pratt). We will also use N-body simulations from the MUSIC project (PI M. de Petris). Notice that key members of the tSZ NIKA2 GT program are deeply involved in these follow-up programs and so we will have direct access to that data.

***Preliminary list of targets***

The current status of the follow-up observations discussed above (not fully finished) does not allow us to present a definitive catalogue of clusters of galaxies. However, using the above criteria and the Planck, ACT, APEX-SZ and CLASH samples we have pre-selected a first sample of clusters of galaxies suitable for our purposes. Notice that for the ACT clusters we do not dispose yet of redshift and we have selected all of them for simplicity. For the CLASH sample, well known disturbed clusters are removed. Furthermore, we consider only clusters that visible with the IRAM 30 m telescopes. Figure 4 shows a mollwide representation of the pre-selected sample, which is detailed in Table 1.

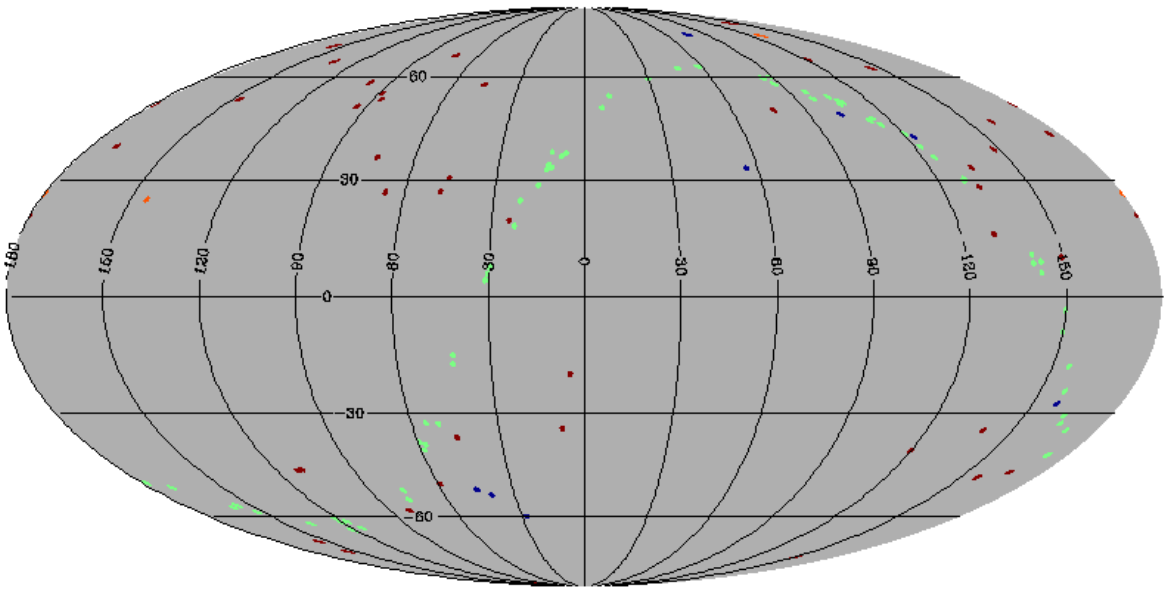


**FIG 4**. Mollwide representation of the selected targets in Galactic coordinates. Planck (red), ACT (green), APEX (blue) and CLASH (orange).

**TABLE 1**. Pre-selected target sample name, equatorial coordinates and redshift.

| *NAME* | *RA* | *DEC* | *z* |
|---|---|---|---|
| PSZ1 G004.45-19.55 | 289.26859 | -33.536189 | 0.540000 |
| PSZ1 G007.55-33.92 | 306.90953 | -34.815597 | 0.550000 |
| PSZ1 G024.20+19.61 | 261.51331 | 1.4797838 | 0.650893 |
| PSZ1 G044.77-51.30 | 333.76547 | -13.987667 | 0.502700 |
| PSZ1 G045.18-36.47 | 320.53850 | -6.8434242 | 0.534400 |
| PSZ1 G045.85+57.71 | 229.58015 | 29.456749 | 0.611000 |
| PSZ1 G046.13+30.75 | 259.25132 | 24.073592 | 0.570000 |
| PSZ1 G048.09+27.18 | 263.56487 | 24.544347 | 0.736080 |
| PSZ1 G058.82-49.66 | 337.05818 | -5.5108580 | 0.520000 |
| PSZ1 G066.41+27.03 | 269.20076 | 40.133093 | 0.569900 |
| PSZ1 G073.22+67.57 | 215.13592 | 39.870316 | 0.566800 |
| PSZ1 G073.64+36.49 | 257.38656 | 47.552579 | 0.560000 |
| PSZ1 G080.66-57.87 | 351.89047 | -2.0616300 | 0.705000 |
| PSZ1 G086.93+53.18 | 228.48655 | 52.797190 | 0.675200 |
| PSZ1 G089.04+55.07 | 224.75191 | 52.826850 | 0.702346 |
| PSZ1 G094.54+51.01 | 227.10387 | 57.889280 | 0.539200 |
| PSZ1 G099.84+58.45 | 213.70036 | 54.778377 | 0.630500 |
| PSZ1 G109.49-45.40 | 3.0666543 | 16.443127 | 0.533998 |
| PSZ1 G110.75-87.48 | 12.276279 | -24.669491 | 0.520000 |
| PSZ1 G111.60-45.72 | 4.6442267 | 16.426146 | 0.545600 |
| PSZ1 G135.24+65.43 | 184.77716 | 50.913083 | 0.527100 |
| PSZ1 G144.86+25.09 | 101.91930 | 70.223162 | 0.584000 |
| PSZ1 G147.86+53.24 | 164.41229 | 58.023665 | 0.600000 |
| PSZ1 G155.25-68.42 | 24.327972 | -8.4782313 | 0.574800 |
| PSZ1 G155.95-72.13 | 22.694978 | -11.831425 | 0.620000 |
| PSZ1 G159.26+71.11 | 178.00986 | 41.564908 | 0.532786 |
| PSZ1 G171.01+39.44 | 132.74845 | 48.491347 | 0.513100 |
| PSZ1 G180.00+51.58 | 149.02485 | 41.135821 | 0.587000 |
| PSZ1 G180.25+21.03 | 109.36717 | 37.743335 | 0.546000 |
| PSZ1 G183.92+42.99 | 137.69662 | 38.802951 | 0.558100 |
| PSZ1 G193.29-46.13 | 53.967809 | -6.9772003 | 0.640000 |
| PSZ1 G199.71+46.53 | 143.47154 | 28.095240 | 0.553387 |
| PSZ1 G201.50-27.34 | 73.533370 | -3.0335377 | 0.537700 |
| PSZ1 G203.17-47.59 | 55.992886 | -13.592428 | 0.575700 |
| PSZ1 G208.61-74.39 | 30.062584 | -24.907828 | 0.720000 |
| PSZ1 G209.80+10.23 | 110.60752 | 7.3955806 | 0.677000 |
| PSZ1 G211.23+38.63 | 137.78469 | 17.773666 | 0.504900 |
| PSZ1 G212.51+63.18 | 163.22504 | 24.196996 | 0.550300 |
| PSZ1 G213.37+80.60 | 182.33817 | 26.663753 | 0.558600 |
| PSZ1 G219.90-34.40 | 73.682892 | -20.288779 | 0.700000 |
| PSZ1 G224.73+33.65 | 137.87591 | 5.8068011 | 0.768200 |
| PSZ1 G226.65+28.43 | 134.13136 | 1.8025289 | 0.724300 |
| PSZ1 G228.21+75.20 | 177.40583 | 22.393133 | 0.545000 |
| PSZ1 G229.08+16.09 | 124.63302 | -6.4050768 | 0.512300 |
| PSZ1 G236.86+66.33 | 170.44496 | 15.829439 | 0.559300 |
| PSZ1 G239.88-39.95 | 71.699130 | -37.013584 | 0.580000 |
| PSZ1 G282.30+49.92 | 179.50911 | -10.798763 | 0.660000 |
| ACTCLJ0008.1+0201 | 2.04180 | 2.02040 | NA |
| ACTCLJ0012.0-0046 | 3.01520 | -0.769300 | NA |
| ACTCLJ0014.9-0057 | 3.72760 | -0.950200 | NA |
| ACTCLJ0017.6-0051 | 4.41380 | -0.858000 | NA |
| ACTCLJ0018.2-0022 | 4.56230 | -0.379500 | NA |
| ACTCLJ0022.2-0036 | 5.55530 | -0.605000 | NA |
| ACTCLJ0026.2+0120 | 6.56990 | 1.33670 | NA |
| ACTCLJ0044.4+0113 | 11.1076 | 1.22210 | NA |

| | | | |
|---|---|---|---|
| ACTCLJ0045.2-0152 | 11.3051 | -1.88270 | NA |
| ACTCLJ0051.1+0055 | 12.7875 | 0.932300 | NA |
| ACTCLJ0058.0+0030 | 14.5189 | 0.510600 | NA |
| ACTCLJ0059.1-0049 | 14.7855 | -0.832600 | NA |
| ACTCLJ0104.8+0002 | 16.2195 | 0.0495000 | NA |
| ACTCLJ0119.9+0055 | 19.9971 | 0.919300 | NA |
| ACTCLJ0127.2+0020 | 21.8227 | 0.346800 | NA |
| ACTCLJ0139.3-0128 | 24.8407 | -1.47690 | NA |
| ACTCLJ0152.7+0100 | 28.1764 | 1.00590 | NA |
| ACTCLJ0156.4-0123 | 29.1008 | -1.38790 | NA |
| ACTCLJ0206.2-0114 | 31.5567 | -1.24280 | NA |
| ACTCLJ0215.4+0030 | 33.8699 | 0.509100 | NA |
| ACTCLJ0218.2-0041 | 34.5626 | -0.688300 | NA |
| ACTCLJ0219.8+0022 | 34.9533 | 0.375500 | NA |
| ACTCLJ0219.9+0129 | 34.9759 | 1.49730 | NA |
| ACTCLJ0221.5-0012 | 35.3925 | -0.206300 | NA |
| ACTCLJ0223.1-0056 | 35.7939 | -0.946600 | NA |
| ACTCLJ0228.5+0030 | 37.1250 | 0.503300 | NA |
| ACTCLJ0230.9-0024 | 37.7273 | -0.404300 | NA |
| ACTCLJ0239.8-0134 | 39.9718 | -1.57580 | NA |
| ACTCLJ0240.0+0116 | 40.0102 | 1.26930 | NA |
| ACTCLJ0241.2-0018 | 40.3129 | -0.310900 | NA |
| ACTCLJ0245.8-0042 | 41.4645 | -0.701300 | NA |
| ACTCLJ0250.1+0008 | 42.5370 | 0.140300 | NA |
| ACTCLJ0256.5+0006 | 44.1354 | 0.104900 | NA |
| ACTCLJ0301.1-0110 | 45.2925 | -1.17160 | NA |
| ACTCLJ0301.6+0155 | 45.4158 | 1.92190 | NA |
| ACTCLJ0303.3+0155 | 45.8343 | 1.92140 | NA |
| ACTCLJ0308.1+0103 | 47.0481 | 1.06070 | NA |
| ACTCLJ0320.4+0032 | 50.1239 | 0.539900 | NA |
| ACTCLJ0326.8-0043 | 51.7075 | -0.731200 | NA |
| ACTCLJ0336.9-0110 | 54.2438 | -1.17050 | NA |
| ACTCLJ0342.0+0105 | 55.5008 | 1.08730 | NA |
| ACTCLJ0342.7-0017 | 55.6845 | -0.289900 | NA |
| ACTCLJ0348.6+0029 | 57.1612 | 0.489200 | NA |
| ACTCLJ0348.6-0028 | 57.1605 | -0.468100 | NA |
| ACTCLJ2025.2+0030 | 306.301 | 0.513000 | NA |
| ACTCLJ2050.5-0055 | 312.626 | -0.931100 | NA |
| ACTCLJ2050.7+0123 | 312.681 | 1.38570 | NA |
| ACTCLJ2051.1+0056 | 312.793 | 0.948800 | NA |
| ACTCLJ2051.1+0215 | 312.789 | 2.26280 | NA |
| ACTCLJ2055.4+0105 | 313.858 | 1.09850 | NA |
| ACTCLJ2058.8+0123 | 314.723 | 1.38360 | NA |
| ACTCLJ2128.4+0135 | 322.104 | 1.59960 | NA |
| ACTCLJ2129.6+0005 | 322.419 | 0.0891000 | NA |
| ACTCLJ2130.1+0045 | 322.537 | 0.759000 | NA |
| ACTCLJ2135.1-0102 | 323.791 | -1.03960 | NA |
| ACTCLJ2135.2+0125 | 323.815 | 1.42470 | NA |
| ACTCLJ2135.7+0009 | 323.931 | 0.156800 | NA |
| ACTCLJ2152.9-0114 | 328.237 | -1.24580 | NA |
| ACTCLJ2154.5-0049 | 328.632 | -0.819700 | NA |
| ACTCLJ2156.1+0123 | 329.041 | 1.38570 | NA |
| ACTCLJ2220.7-0042 | 335.192 | -0.709500 | NA |
| ACTCLJ2229.2-0004 | 337.304 | -0.0743000 | NA |
| ACTCLJ2253.3-0031 | 343.343 | -0.528000 | NA |
| ACTCLJ2302.5+0002 | 345.643 | 0.0419000 | NA |
| ACTCLJ2307.6+0130 | 346.918 | 1.51610 | NA |
| ACTCLJ2327.4-0204 | 351.866 | -2.07770 | NA |
| ACTCLJ2337.6+0016 | 354.416 | 0.269000 | NA |
| ACTCLJ2351.7+0009 | 357.935 | 0.153800 | NA |

| | | | |
|---|---|---|---|
| MS0451.6-0305 | 4.9031389 | -3.0146111 | 0.550000 |
| XMMXCSJ095940.8+023111.3 | 9.9946667 | 2.5198056 | 0.720000 |
| MS1054.4-0321 | 10.949722 | -3.6269444 | 0.830000 |
| XMMUJ1230.3+1339 | 12.504694 | 13.651194 | 0.975000 |
| RDCSJ1252-2927 | 12.881778 | -29.454722 | 1.24000 |
| RXCJ2214.9-1359 | 22.249278 | -14.003000 | 0.503000 |
| XMMXCSJ2215.9-1738 | 22.266111 | -17.634028 | 1.45000 |
| XMMUJ2235.3-2557 | 22.589056 | -25.961667 | 1.39300 |
| MACSJ0744.9+3927 | 7.7480056 | 39.457472 | 0.686000 |
| MACSJ1149.5+2223 | 11.826581 | 22.398500 | 0.544000 |
| MACSJ0647.7+7015 | 6.7972972 | 70.248611 | 0.584000 |

***Few extra issues***

Some main issues need to be addressed in further detail:

1) to have a cosmological representative catalogue we would like to have an homogeneous distribution in redshift in order to separate the cluster sample in various redshift bins. A compromise must be reached in the final catalogue
2) known disturb clusters are removed from the sample but we can still have unknown ones in the selected sample. A careful study and extra selection must be undertaken a posteriori
3) a simulation study needs to be carried out to predict the expected tSZ signal to optimize the observation time
4) extensions of the sample can be imagined in various ways depending on the final mapping speed. We can imagine for example to include disturb systems, to low the redshift threshold to have some overlap with previous studies, etc
5) the final sample will include backup clusters

## 5. Observing strategy

We plan to perform OTF scans for each cluster individually. The size of the OTF map will be tuned to the expected angular size of the cluster. As discussed above most observed clusters are expected to have angular sizes between 6 and 10 arcmin, thus we expect to use maps of 10 x 10 arcmin. This is to maximize the on source time and minimize the observing time while preserving large angular scales. Taking into account previous NIKA experience on tSZ observations we will perform OTF scans in various different orientations to improve atmospheric noise removal.

The expected typical on source integration per cluster is about 4 hours. Assuming 50 targets, this is equivalent to 200 hours on source for a total program of 300 hours including overheads. This will allow us to reach at 140 (260) GHz a sensitivity of 5 (30) x$10^{-5}$ in Compton parameter units across a10x10 arcmin field. This can be better observed in Figure 5.

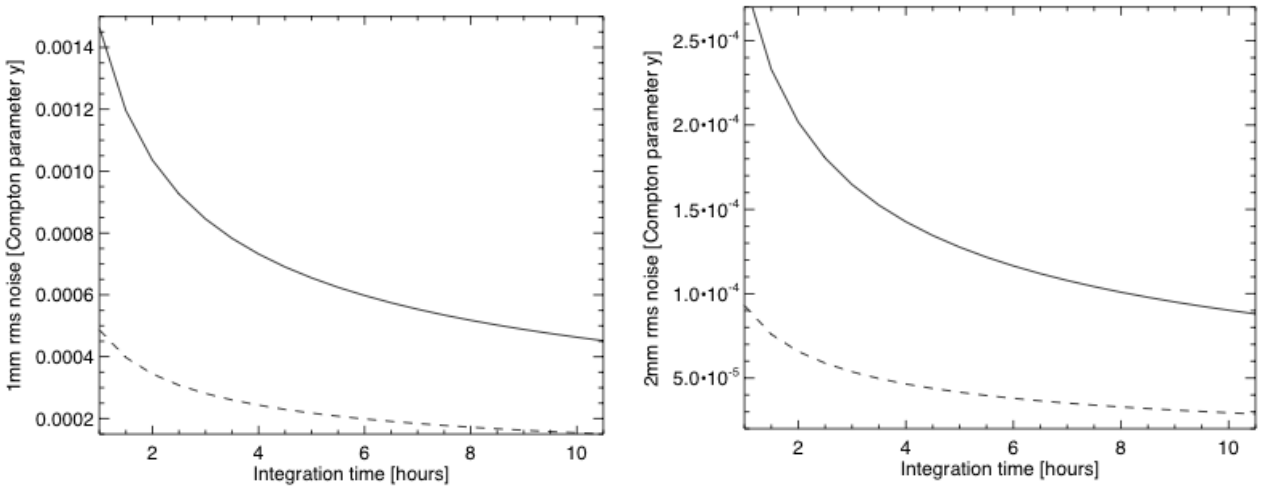

**FIG 5.** rms noise per beam in Compton parameter units for a patch of 10 x 10 arcmin as function of integration time in hours for the 260 (left) and 140 (right) GHz bands. Goal and specifications sensitivities are presented in dashed and solid lines respectively.

Reducing the map size to 7x7 arcmin we can improve the sensitivity by a factor of about 2 and thus reach a sensitivity of about $2.5 \times 10^{-5}$ . This can be used to obtain reliable observations of the faintest clusters. Alternatively, we can keep the same sensitivity reducing the integration time by factor of  and so allowing for the observation of a larger number of targets.

In the case the sensitivity is at specification values rather than the goal ones we will simply limit the observing regions and/or the number of observable targets to keep the 200 hours of on source integration time.

**6. References**